

Multiantenna Artificial Photosynthetic Reaction Center Complex

Yuichi Terazono, Gerdenis Kodis, Paul A. Liddell, Vikas Garg, Thomas A. Moore,*
Ana L. Moore,* and Devens Gust*

Department of Chemistry and Biochemistry, Center for Bioenergy and Photosynthesis, Arizona State University,
Tempe, Arizona 85287-1604

Received: January 28, 2009; Revised Manuscript Received: April 3, 2009

In order to ensure efficient utilization of the solar spectrum, photosynthetic organisms use a variety of antenna chromophores to absorb light and transfer excitation to a reaction center, where photoinduced charge separation occurs. Reported here is a synthetic molecular heptad that features two bis(phenylethynyl)anthracene and two borondipyrromethene antennas linked to a hexaphenylbenzene core that also bears two zinc porphyrins. A fullerene electron acceptor self-assembles to both porphyrins via dative bonds. Excitation energy is transferred very efficiently from all four antennas to the porphyrins. Singlet–singlet energy transfer occurs both directly and by a stepwise funnel-like pathway wherein excitation moves down a thermodynamic gradient. The porphyrin excited states donate an electron to the fullerene with a time constant of 3 ps to generate a charge-separated state with a lifetime of 230 ps. The overall quantum yield is close to unity. In the absence of the fullerene, the porphyrin excited singlet state donates an electron to a borondipyrromethene on a slower time scale. This molecule demonstrates that by incorporating antennas, it is possible for a molecular system to harvest efficiently light throughout the visible from ultraviolet wavelengths out to ~650 nm.

Introduction

In photosynthetic organisms, most of the sunlight is absorbed by antenna pigment–protein complexes, rather than by the reaction center that converts excitation energy to electrochemical potential. Antenna systems are also of interest in the design and construction of artificial photosynthetic complexes, wherein synthetic molecules use the basic photochemistry and photophysics of photosynthesis to carry out solar energy conversion. Chlorophylls are major constituents of natural antenna systems, and a wide variety of synthetic antennas based on porphyrins or other cyclic tetrapyrroles have been prepared.^{1–19} We have previously reported examples of artificial photosynthetic antenna–reaction center complexes where porphyrin arrays absorb light and transfer it to porphyrin–fullerene units wherein photoinduced electron transfer takes place.^{1,2}

Although porphyrins and chlorophylls offer many advantages as antenna chromophores, they do not absorb strongly throughout the range of wavelengths useful for photosynthesis. As a result, photosynthetic organisms employ other chromophores, such as carotenoids, phycoerythrins, and phycocyanins, in order to approach full spectral coverage. In addition to studies of carotenoid antennas in artificial photosynthesis,^{20–24} we recently reported the synthesis and study of a heptad molecule in which five bis(phenylethynyl)anthracene (BPEA) antenna chromophores and a porphyrin–fullerene artificial reaction center were organized by a hexaphenylbenzene core.^{25,26} In the heptad, both the porphyrin and the BPEA units absorb light that ultimately gives rise to photoinduced electron transfer and formation of a charge-separated state. Although light absorption in part of the visible region is enhanced relative to systems with only porphyrins as antennas, light gathering was still inefficient in some spectral ranges.

We now report the preparation and study of heptad **1** (Figure 1), a partially self-assembled antenna–reaction center complex that features strong absorption throughout the visible. The two zinc porphyrin moieties attached to the hexaphenylbenzene coordinate a fullerene electron acceptor that bears two pyridine ligation units. The hexaphenylbenzene core also supports two BPEA antennas that absorb in the 400–500 nm region, and two borondipyrromethene (BDPY) chromophores with absorption in the 450–550 and 330–430 nm ranges. As demonstrated below, both kinds of antennas efficiently transfer singlet excitation energy to the porphyrin, which donates an electron to the fullerene to generate a charge-separated state.

Results

Synthesis. Heptad **1** self-assembles from hexad **2** and the previously reported²⁷ fullerene **3**. Key steps in the preparation of **2** include the Diels–Alder reaction of the appropriately substituted tetraphenylcyclopentadienone and porphyrin-linked diphenylacetylene to yield a hexaphenylbenzene core bearing the two porphyrins. The BPEA units were synthesized and then added to the core via copper-free Sonogashira coupling chemistry, and finally the BDPY antennas were built up on the hexaphenylbenzene framework. The details of the synthesis of **2** and the various model compounds discussed below are described in the Supporting Information, along with the characterization of intermediate compounds and final products using NMR and mass spectrometry.

Spectroscopic results. The photochemistry and photophysics of **1** and **2** are sufficiently complex that understanding them required the study of a variety of model compounds. We will begin by describing the results for hexad **2** and associated model compounds. Next, we will report results for heptad **1**. Finally, we will summarize the results of these studies in terms of a model for the photochemistry of the heptad.

* To whom correspondence should be addressed. E-mail: (D.G.) gust@asu.edu; (T.A.M.) tom.moore@asu.edu; (A.L.M.) amoore@asu.edu.

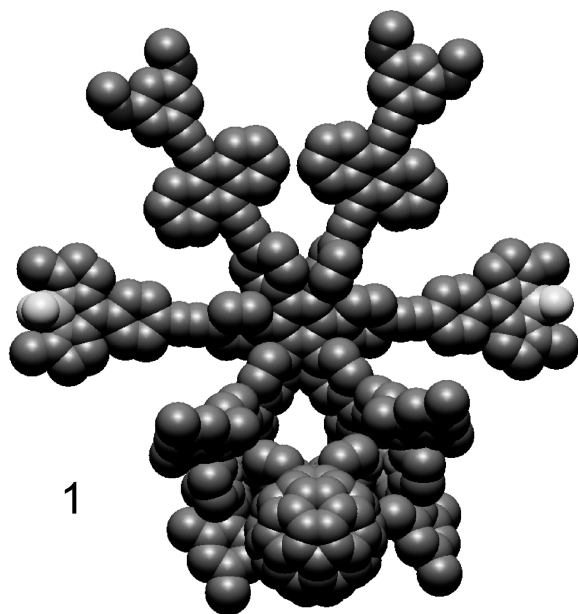


Figure 1. Molecular model of self-assembled heptad **1** and components hexad **2** and fullerene derivative **3**. The free base porphyrin analog of **2** is designated **7**.

Absorption and Emission Properties of the Hexad and Model Compounds in 2-Methyltetrahydrofuran. Figure 2 shows the absorption (a) and fluorescence emission (b) spectra in 2-methyltetrahydrofuran of model BPEA chromophore **4**, model BDPY **5**, and dyad **6**, which features one BPEA and one BDPY unit ortho to one another on a hexaphenylbenzene core. The corresponding structures are shown in Figure 3. The BPEA antenna features absorbance maxima at 309, 319, 445, and 469 nm and emission maxima at 483, 515 and \sim 547 (sh) nm. As reported earlier,²⁵ the fluorescence quantum yield in 2-methyltetrahydrofuran is 0.94, and the lifetime of the first excited singlet state is 2.80 ns. The energy of the excited state,

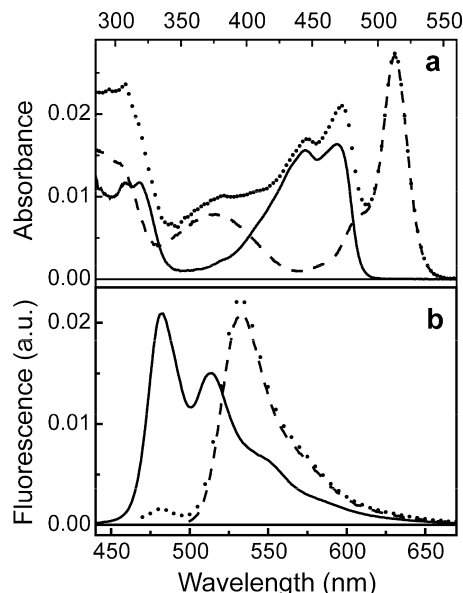


Figure 2. Absorption (a) and fluorescence emission ($\lambda_{\text{ex}} = 400$ nm) (b) spectra of model BPEA chromophore **4** (—), model BDPY **5** (---), and BPEA-BDPY dyad **6** (···) in 2-methyltetrahydrofuran.

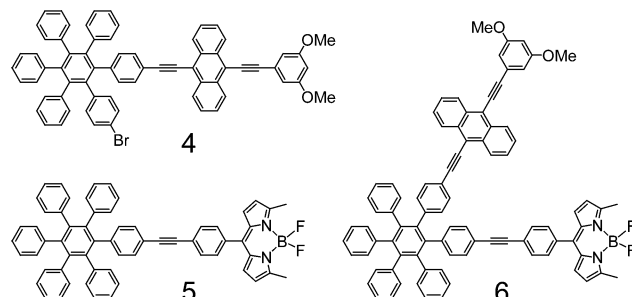


Figure 3. Structures of model BPEA chromophore **4**, model BDPY **5**, and BPEA-BDPY dyad **6**.

estimated from the wavenumber average of the longest-wavelength absorption maximum and shortest-wavelength emission maximum, is 2.61 eV. In the same solvent, the model BDPY **5** has absorption maxima at \sim 300, 376, 487 (sh), and 513 nm (Figure 2a). The emission maxima are at 534 and \sim 563 (sh) nm (Figure 2b). The fluorescence quantum yield of **5** was determined to be 0.04, using the comparative method with Rhodamine 6G ($\Phi = 0.90$ in water²⁸) as the standard.

Dyad **6**, which features both antenna types, has an absorption spectrum similar to a linear combination of the spectra of models **4** and **5** with no significant perturbations due to inclusion of both moieties in the same molecule (Figure 2a). The emission spectrum of **6** with excitation at 400 nm (Figure 2b) closely resembles that of **5**. Given the difference in quantum yields of fluorescence for **4** and **5**, it is clear in the dyad that the first excited singlet state of BPEA is strongly quenched by the nearby BDPY.

Figure 4a shows the absorption spectra in 2-methyltetrahydrofuran of the free base form of hexad **2** (designated **7**), which lacks a fullerene electron acceptor, along with those of model porphyrin dyad **8** and BDPY-porphyrin dyad **10** (Figure 5). The porphyrin dyad **8** has absorption maxima at \sim 400 (sh), 418 (Soret), \sim 425 (sh), 514, 546, 593, and 649 nm. The Q-band maxima are virtually unchanged from those of a model free-base porphyrin monomer, showing that there are no strong interactions between the two porphyrins. When comparing the spectra of **8** and **10**, a small excitonic splitting of the porphyrin

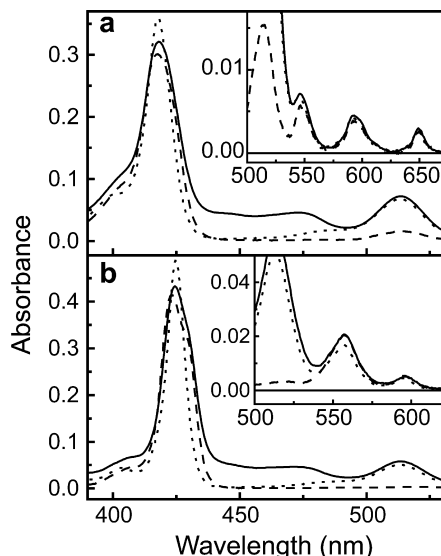


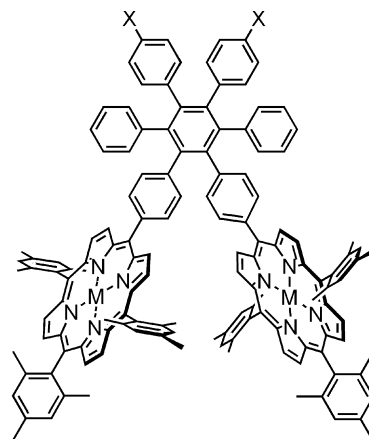
Figure 4. Absorption spectra in 2-methyltetrahydrofuran of (a) free base porphyrin hexad **7** (—), free base porphyrin dyad **8** (---), and BDPY-free base porphyrin dyad **10** (····) and (b) zinc porphyrin hexad **2** (—), zinc porphyrin dyad **9** (---), and BDPY-zinc porphyrin dyad **11** (····). The insets show the longer-wavelength spectral regions in expanded form.

Soret band can be seen in **8**. Attachment of a BDPY antenna ortho to a porphyrin on the hexaphenylbenzene core (**10**) gives rise to new maxima at 300, 372 (not shown in Figure 4a), and ~485 (sh) nm, superimposed on the same porphyrin absorption bands as were observed for **8**. Finally, Figure 4a also shows that the spectrum of hexad **7** displays maxima at 308, ~372 (sh), ~400 (sh), 418, ~425 (sh), 445, 473, 514, 546, 593, and 649 nm. The spectrum is close to a linear combination of the spectra of all six chromophores. It will be noted that the four antenna units add considerable absorption in the 430–550 nm region but have virtually no effect on the two longest-wavelength porphyrin Q-bands.

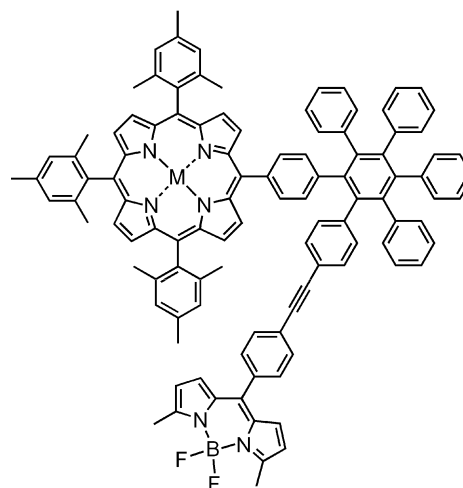
Figure 4b shows spectra taken under comparable conditions for the corresponding zinc compounds: hexad **2**, porphyrin dyad **9**, and BDPY-porphyrin dyad **11**. Dyad **9** features maxima at ~405 (sh), 425, ~430 (sh), 557, and 598 nm. The spectrum is typical of zinc tetra-arylporphyrins with the addition of a small excitonic splitting of the Soret band that features a larger oscillator strength for the shorter-wavelength transition. Similar splitting has been observed in closely related compounds.²⁷ The BDPY-porphyrin dyad **11** lacks this excitonic splitting, showing maxima at 300, 372, ~405(sh), 425 (Soret), ~485(sh), 513, 557, and 598 nm. However, new maxima due to absorption by BDPY are observed, as was the case for **10**. Hexad **2** displays maxima at 308, ~372(sh), ~405(sh), 425, ~430(sh), 445, 473, 514, 557, and 598 nm and represents a superposition of the spectra of the chromophores of dyad **9**, two BDPY units, and two BPEA chromophores.

The fluorescence spectra of free base compounds **7**, **8**, and **10** in 2-methyltetrahydrofuran all show typical porphyrin emission at 650 and 721 nm. Zinc analogs **2**, **9**, and **11** display typical zinc porphyrin emission at 600 and 654 nm, but the emission in **2** and **11** is quenched relative to that from **9**. This quenching must be due to the presence of the BDPY units (vide infra).

Time-Resolved Absorption and Emission Properties of the Hexad and Model Compounds in 2-Methyltetrahydrofuran. The time-dependent spectroscopic properties of the hexads and models were studied in 2-methyltetrahydrofuran at ambient



8: M = 2H, X = H
9: M = Zn, X = H
18: M = Zn, X = Br



10: M = 2H
11: M = Zn

Figure 5. Structures of free base and zinc forms of porphyrin dyads (**8**, **9**) and BDPY-porphyrin dyads (**10**, **11**).

temperatures using pump–probe transient absorption, fluorescence upconversion, and single-photon-timing emission experiments. Details of the spectroscopic methods are given in the Supporting Information.

BPEA-BDYP Dyad **6** and Relevant Model Compounds.

The model BDPY chromophore **5** was found by all three methods to have a singlet excited-state lifetime of ~260 ps. At shorter time scales, transients ascribed to excited-state solvation and ground-state equilibration effects with time constants of 2–3 and 11 ps were observed (see Supporting Information). Relaxation dynamics on similar time scales have also been reported for related BDPY systems and related theoretically to rotation about the single bond joining the boron heterocycle to the phenyl ring.^{29,30}

As mentioned above, the lifetime of ¹BPEA in **4** is 2.80 ns. Similar studies on dyad **6** (Figure 6a) show that the decay of ¹BPEA is multiexponential but can be fitted with time constants of 4.7 ps (43%) and 14 ps (57%). The great reduction in lifetime relative to that of **4** is due to very rapid singlet–singlet energy transfer to BDPY. The multiexponential behavior is ascribed to the presence of a variety of energy-accepting conformations for BDPY. The transition dipole moment for BDPY is located along the longest axis of the boron heterocycle, and intercon-

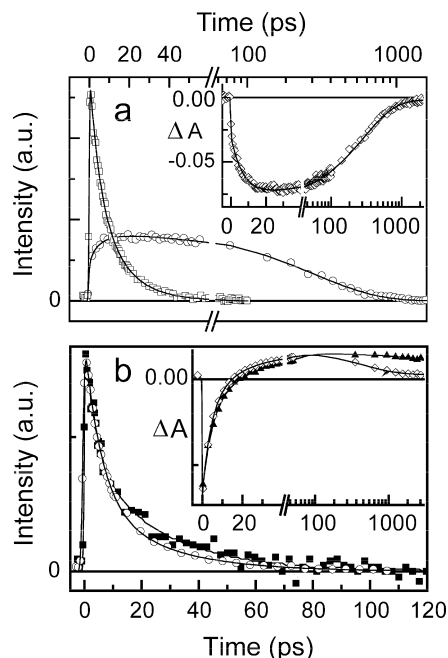


Figure 6. (a) Fluorescence decay kinetics of BDPY-BPEA dyad **6** at 490 nm (squares) and 600 nm (circles) with excitation at 430 nm. Fitting as two exponentials gives time constants of 4.7 ps (43%) and 14 ps (57%) at 490 nm and 7.1 ps (rise) and 281 ps at 600 nm. The inset shows transient absorption kinetics of **6** at 510 nm following excitation at 455 nm. Fitting gives time constants of 7.4 ps (rise) and 285 ps, plus 5% of a nondecaying component. (b) Intensity-normalized fluorescence decay kinetics of BDPY-free base porphyrin **10** (squares) and BDPY-zinc porphyrin **11** (hollow circles) at 570 and 540 nm, respectively ($\lambda_{ex} = 430$ nm). Two-exponential fits (lines) give 5.2 ps (59%) and 24 ps (41%) for **10** and 5.1 ps (62%) and 19.6 ps (38%) for **11**. The inset shows normalized transient absorption kinetics of **10** (triangles) and **11** (hollow diamonds) at 540 nm ($\lambda_{ex} = 505$ nm). Exponential fitting gives 4.9 ps (62%), 23.2 ps (38%), and nondecaying components for **10**. Kinetics for **11** show 4.3 ps (64%), 19.4 ps (36%), and 450 ps (decay of induced absorption, fixed in the analysis).

version of various conformations arising from rotation around the bonds joining this heterocycle to the hexaphenylbenzene core is postulated to be slower than the observed energy transfer rates and will change the mutual orientations of the BPEA energy donor and BDPY acceptor transition moments. Calculations using the Förster equation³¹ show that such variations are consistent with the observed range of transfer rates. The BDPY excited-state decays with a time constant of 280 ps, which is slightly larger than that observed for model **5**. Thus, ¹BDPY is unquenched.

BDPY-Porphyrin Dyads. Figure 6b shows BDPY fluorescence decay kinetics for dyads **10** and **11** at 570 and 540 nm, respectively, with excitation at 430 nm, and (inset) the decay of BDPY stimulated emission at 540 nm following excitation at 505 nm. All these emission decays were satisfactorily fitted with two time constants. For free base **10**, the results were 5.2 ps (59%) and 24 ps (41%) from fluorescence and 4.9 ps (62%) and 23.2 ps (38%) from stimulated emission. In zinc dyad **11**, the lifetimes were 5.1 ps (62%) and 19.6 ps (38%) from fluorescence and 4.3 ps (64%) and 19.4 ps (36%) from stimulated emission. The short BDPY lifetimes, relative to the 257 and 280 ps lifetimes found in **5** and **6**, are due to rapid singlet–singlet energy transfer from BDPY to the porphyrin. The multiexponential nature of these decays is attributed to the presence of several conformations of ¹BDPY relative to the porphyrin energy acceptors, which give rise to different time constants for energy transfer. Multiexponential singlet energy

transfer from BDPY chromophores to porphyrins has been observed by other researchers.³⁰ The data in Figure 6 (inset) also yield information concerning the lifetimes of the porphyrin excited singlet states. The lifetime of BDPY-¹P in **10** was too long to measure using the pump–probe apparatus, but fluorescence experiments using the single-photon-timing method ($\lambda_{ex} = 290$ nm) yielded a single-exponential emission ($\chi^2 = 1.02$) at 650 nm with a lifetime of 10.5 ns, which is typical for a free base porphyrin of this general type.

The lifetime of BDPY-¹P_{Zn} in **11** was found to be only 450 ps, based on the data in the inset of Figure 6 and single-photon-timing experiments at 650 nm ($\lambda_{ex} = 290$ nm, $\chi^2 = 1.09$). The lifetime of the zinc porphyrin first excited singlet state of a dyad very closely related to **9** is 2.2 ns.²⁷ The quenching in **11** is ascribed to photoinduced electron transfer from the porphyrin to BDPY to yield BDPY^{•−}-P_{Zn}^{•+}. This was confirmed by nanosecond transient absorption experiments with excitation at 595 nm and detection at 460 (to monitor the induced absorption of, mainly, P_{Zn}^{•+}) and 500 nm (to monitor BDPY^{•−}) (see Supporting Information). These data showed a lifetime for BDPY^{•−}-P_{Zn}^{•+} of 4.8 ns. An additional component, which did not decay on the time scale of this measurement, was assigned to the triplet state of the porphyrin.

Hexads. The excited-state properties of free base BPEA-BDPY-P hexad **7** and zinc analog **2** were investigated in 2-methyltetrahydrofuran using the same techniques. Fluorescence decay measurements on **7** with excitation at 430 nm and detection at 490 nm, where BPEA emits, gave a lifetime for ¹BPEA of 2 ps for 94% of the decay (see Supporting Information). Detection at 570 nm, where emission is from both BPEA and BDPY, gave a multiexponential decay that was fitted satisfactorily with lifetimes of 3 ps (68%) and 20 ps (32%). This is ascribed to decay of multiple ¹BDPY conformations by singlet energy transfer to the porphyrin, as was observed for **10**, and a small contribution from ¹BPEA. The lifetimes of ¹BDPY observed in **7** are very slightly shorter than those observed for dyad **10**. This may reflect a small amount of energy transfer to the porphyrin meta to the BDPY in addition to transfer to the ortho porphyrin. Single-photon-timing fluorescence decay measurements at 650 nm for **7** yielded a lifetime for the porphyrin first excited singlet state of 9.4 ns, which indicates no significant quenching of ¹P.

The lifetimes of ¹BDPY and ¹P in free base hexad **7** are similar to those found for model compound **10**. However, the lifetime of ¹BPEA (2 ps) is reduced relative to that observed in **6** (5–14 ps), indicating a pathway for decay of ¹BPEA in addition to singlet energy transfer to the BDPY unit. Our earlier studies of BPEA-porphyrin moieties arranged on a hexaphenylbenzene core,²⁵ carried out with dyads **12**, **13**, and **15** (Figure 7), have shown that in an arrangement such as that in **7**, the BPEA units can exchange excitation energy with each other with $\tau = 0.4$ ps, and transfer singlet excitation energy to free base porphyrins in meta ($\tau = 8$ ps) and para (4 ps) relationships. Thus, in hexad **7**, the BPEA units can decay by three different singlet energy transfer pathways. If we take the average lifetime for ¹BPEA in **6** as 10 ps, then the reciprocal of the sum of the decay rates for the three pathways is 2.1 ps, which is essentially identical to the measured 2 ps time constant.

The results for zinc hexad **2** are slightly more complex due to the occurrence of photoinduced electron transfer from the zinc porphyrin excited-state to BDPY. Measurements analogous to those discussed above gave a lifetime for the BPEA units of 2 ps, which is similar to that found with the free base system. Fluorescence decay-associated spectra (DAS) for **2** were

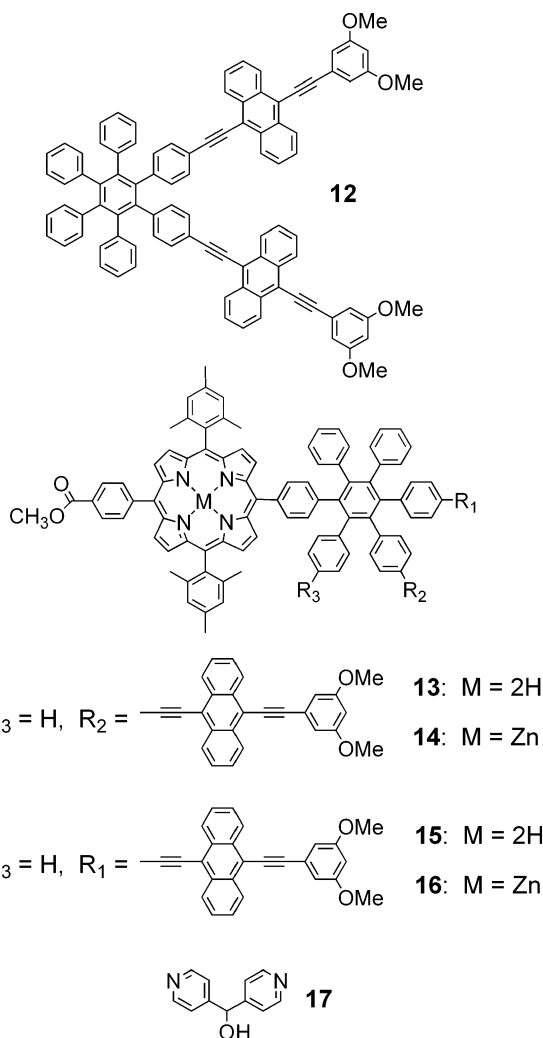


Figure 7. Structures of BPEA dyad **12** and model BPEA-porphyrin dyads **13**, **14**, **15**, and **16**.

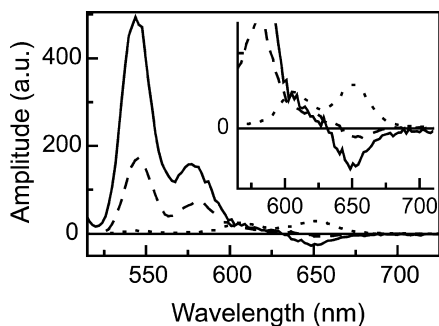


Figure 8. Hexad **2** fluorescence decay-associated spectra with time constants of 2.2 ps (—), 15.6 ps (---), and 450 ps (···) (fixed in the analysis) with excitation at 480 nm. The inset is an expansion of the long-wavelength part of the spectra. The DAS show some distortion at shorter wavelengths due to fluorescence reabsorption by other chromophores and are not corrected for streak camera spectral response.

obtained by means of the time-resolved fluorescence streak camera technique with excitation at 480 nm (Figure 8). Global analysis gave spectral components with lifetimes of 2.2, 15.6, and 450 ps. The spectrum of the 2.2 ps component in the 500–600 nm region is consistent with decay of ¹BPEA by energy transfer to BDPY and P_{Zn}. The negative amplitude around 650 nm represents the rise of P_{Zn} fluorescence due to the energy transfer. The 2.2 ps time constant is consistent with

TABLE 1: Time Constants for Photochemical Processes (ps)

| process | free base 7 | hexad 2 | | heptad 1 |
|---------|----------------------|----------------------|----------------------|----------------------|
| | 2-meTHF ^a | 2-meTHF ^a | 1,2-DFB ^b | 1,2-DFB ^c |
| step 1 | 0.4 | 0.4 | 0.4 ^d | 0.4 |
| step 2 | 5–14 | 5–14 | 5–13 | 5–13 |
| step 3 | 8 | 7 | 7 ^d | 7 |
| step 4 | 4 | 6 | 6 | 6 |
| step 5 | 5–24 | 4–20 | 2–15 | 2–15 |
| step 6 | | 570 | 230 | 230 |
| step 7 | | 4800 | 1500 | 1500 |
| step 8 | | | | 3 |
| step 9 | | | | 230 |

^a 2-Methyltetrahydrofuran. ^b 1,2-Difluorobenzene containing excess ligand **17**. ^c 1,2-Difluorobenzene containing excess ligand **3**. ^d Estimated from results in 2-methyltetrahydrofuran.

the values of 5 and 14 ps found for transfer to BDPY in dyad **6** combined with time constants of 7 and 6 ps for transfer from BPEA to zinc porphyrins meta and para to it, as found previously²⁵ for dyads **14** and **16**. Similarly, the 15.6 ps DAS shows energy transfer from ¹BDPY to P_{Zn}. The 450 ps DAS has the shape of porphyrin emission. The time constant could not be extracted from these short time scale streak camera data but was determined to be 450 ps from single-photon-timing fluorescence measurements and was fixed at this value for the analysis. This value is identical to that obtained in **11** for photoinduced electron transfer from ¹P_{Zn} to BDPY and is ascribed to the same process.

Transient absorption evolution-associated difference spectra (EADS) were also obtained for hexad **2**, and the results are consistent with the above analysis. As discussed in the Supporting Information, EADS are obtained by global analysis of the transient absorption data over a wide range of wavelengths. A kinetic model consisting of sequentially interconverting species, each of which decays monoexponentially, is used. The result is a group of spectra, each associated with one of the exponential lifetimes. Although each EADS does not usually portray the spectrum of a pure chemical state or species, the set of spectra enable a clearer picture of the evolution of the system than can be obtained from the raw kinetic data. In the case of hexad **2**, the EADS yielded a lifetime for the BDPY^{•-}-P_{Zn}^{•+} state that was consistent with the 4.8 ns lifetime obtained for the corresponding state in **11**.

From the results described above, we can summarize the relevant photophysics for the hexads in 2-methyltetrahydrofuran (Table 1). This is most easily done with reference to Figure 9, which shows the various energy and electron transfer pathways for the final heptad system. After light absorption by a BPEA antenna chromophore, singlet energy is exchanged with the neighboring BPEA (step 1) with a time constant of 0.4 ps. Transfer to BDPY, step 2, occurs with $\tau = 5\text{--}14$ ps, due to multiple conformations of BDPY. All of these time constants are essentially identical for the zinc and free base forms of the hexads. The BPEA moieties also transfer excitation energy directly to the porphyrins meta (step 3) and para (step 4) to them with time constants of 8 and 4 ps for free base hexad **7** and 7 and 6 ps for zinc molecule **2**. Excited BDPY, whether generated by light absorption or energy transfer from BPEA, decays by energy transfer to the porphyrin (step 5). Time constants of $\sim 5\text{--}24$ ps are assigned for this process in **7**, and the time constants are very similar (4–20 ps) for hexad **2**. Overall, in both hexads the quantum yield of energy transfer from the various antenna chromophores to the porphyrins is very high. The exact yield is slightly wavelength dependent.

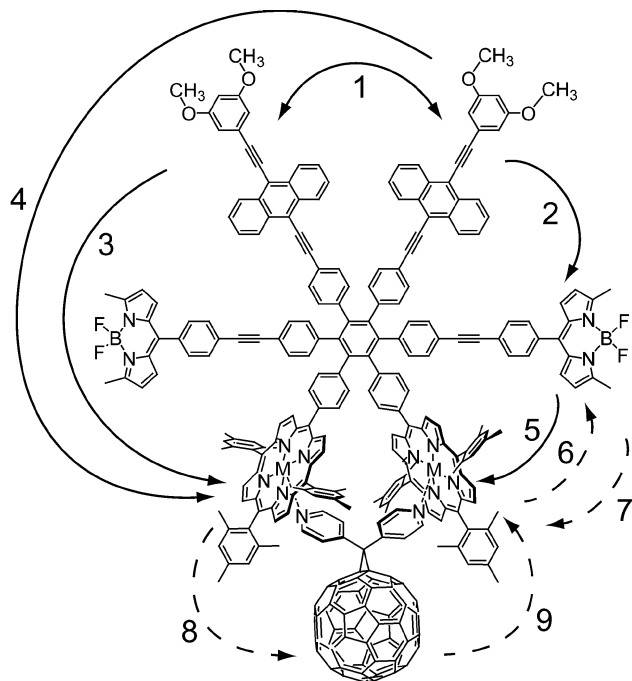


Figure 9. Singlet excitation energy (—) and electron (---) transfer pathways observed in heptad **1** and model compounds. The associated time constants are reported in Table 1.

The yield of excitation transfer from the BPEA units and most efficient conformations of the BDPY to the porphyrins is essentially unity, whereas that from the less efficient BDPY conformations is $\sim 93\%$.

The first excited singlet state lifetimes of the free base porphyrins in **7** are unaffected by the surrounding chromophores, but in zinc hexad **2**, photoinduced electron transfer to the BDPY occurs with $\Phi = 0.80$ to yield a charge-separated state with a lifetime of 4.8 ns. As will be shown in the next section, this process is insignificant in the full heptad **1** because photoinduced electron transfer to the fullerene is much more rapid.

Spectroscopic Properties of Hexads and Model Compounds in 1,2-Difluorobenzene. The formation of heptad **1** requires complexation of dipyrindyl fullerene derivative **3** with hexad **2**. The binding constant for this one-to-one association, as measured in a very closely related system,²⁷ is $7.3 \times 10^4 \pm 3 \times 10^3 \text{ M}^{-1}$ in 1,2-difluorobenzene but is significantly lower in more highly coordinating solvents that compete for the zinc binding sites, including 2-methyltetrahydrofuran. For this reason, we studied the spectroscopic properties of hexad **2** and model compounds in 1,2-difluorobenzene using the same methodologies as described above.

Single photon timing fluorescence experiments ($\lambda_{\text{ex}} = 430 \text{ nm}$) with model BPEA dyad **12** and model BDPY **5** yielded excited singlet state lifetimes in 1,2-difluorobenzene of 2.96 ns ($\lambda = 490 \text{ nm}$, $\chi^2 = 1.02$) and 340 ps ($\lambda = 560 \text{ nm}$, $\chi^2 = 1.11$), respectively. Fluorescence upconversion studies of BDPY-BPEA dyad **6** with excitation mainly into BPEA ($\lambda_{\text{ex}} = 430 \text{ nm}$) showed decay time constants of 4.7 ps (43%) and 12.5 ps (57%) at 490 nm where the BPEA emits, and 4.9 ps (rise) and 360 ps at 570 nm where emission is mainly from BDPY (see Supporting Information). These data are interpreted as indicating singlet-singlet energy transfer from BPEA to BDPY with multiple time constants ($\sim 5\text{--}13 \text{ ps}$) due to multiple BDPY conformations, as found in 2-methyltetrahydrofuran. The BDPY singlet state lifetime, 360 ps, is slightly increased relative to that in model **5**.

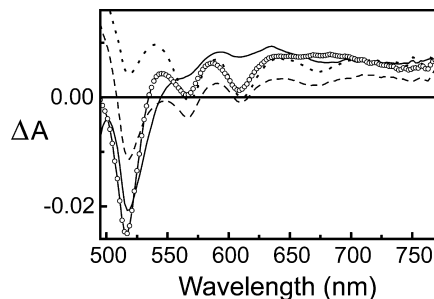


Figure 10. Evolution associated difference absorption spectra (EADS) of a solution of **2** in 1,2-difluorobenzene containing an excess of complexing dipyrindyl compound **17** ($\lambda_{\text{ex}} = 480 \text{ nm}$). Global analysis gives lifetimes of 2.6 ps (solid line), 13.6 ps (dashed line), 210 ps (dotted line), and $\sim 1 \text{ ns}$ (hollow circles).

Transient absorption measurements on BPEA-porphyrin dyad **16** ($\lambda_{\text{ex}} = 480 \text{ nm}$, see Supporting Information) gave EADS that showed singlet-singlet energy transfer from BPEA to the zinc porphyrin with a time constant of 5.8 ps and a porphyrin-excited singlet state lifetime of 2.2 ns. The energy transfer time constant is virtually identical to that measured in 2-methyltetrahydrofuran (5.7 ps). For this reason, similar experiments were not carried out on **14**, and an energy transfer time constant of $\sim 7 \text{ ps}$ was assumed for this molecule by analogy to the 2-methyltetrahydrofuran results.

Transient absorption experiments with BDPY-porphyrin dyad **11** ($\lambda_{\text{ex}} = 480 \text{ nm}$, see Supporting Information) were also performed. For these experiments, excess model pyridine ligand **17** was added to the solution so that the porphyrin was present in the ligated form. This was done because the absorption spectra and redox properties of zinc porphyrins are known to change slightly upon pyridine ligation.³² Global analysis of the data gave satisfactory results with four EADS. The first two EADS (1.9 and 15 ps) reflect a two-exponential fit to multiexponential singlet-singlet energy transfer from BDPY to the zinc porphyrin due to conformational heterogeneity. The third EADS shows zinc porphyrin excited-state quenching by photoinduced electron transfer to BDPY ($\tau = 210 \text{ ps}$) to yield $\text{BDPY}^{\cdot-}\text{-P}_{\text{Zn}}^{+\cdot}$, which decays with a time constant of 1.5 ns (final EADS).

Transient absorption measurements were also performed on hexad **2** in 1,2-difluorobenzene in the presence of excess **17** ($\lambda_{\text{ex}} = 480 \text{ nm}$), and the resulting EADS appear in Figure 10. Global analysis gave a satisfactory fit to the data with four time constants: 2.6 ps, 13.6 ps, 201 ps, and $\sim 1 \text{ ns}$. The spectral shapes of the EADS indicate that the 2.6 and 13.6 ps components are both associated with singlet energy transfer from $^1\text{BPEA}$ to BDPY and from both $^1\text{BPEA}$ and $^1\text{BDPY}$ to the porphyrin. These time constants are consistent with the results for the various model compounds discussed above. The 210 ps spectrum indicates quenching of $^1\text{P}_{\text{Zn}}$ from its usual lifetime of 2.2 ns due to photoinduced electron transfer from the zinc porphyrin to BDPY, and the $\sim 1 \text{ ns}$ spectrum represents decay of $\text{BDPY}^{\cdot-}\text{-P}_{\text{Zn}}^{+\cdot}$.

The results for hexad **2** in 1,2-difluorobenzene are summarized in Table 1. The numbers in the table are based on the results described above for **2** and the various model compounds. The energy transfer behavior is very similar to that in 2-methyltetrahydrofuran. The quantum yields of energy transfer from the BPEA antennas and the most efficient conformations of BDPY to the zinc porphyrin are essentially unity, whereas that from the less efficient conformations of BDPY is $\sim 96\%$. The quantum yield of photoinduced electron transfer from the porphyrin excited-state to yield $\text{BDPY}^{\cdot-}\text{-P}_{\text{Zn}}^{+\cdot}$ is 91%.

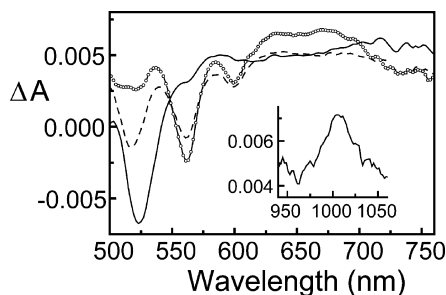


Figure 11. Evolution associated difference absorption spectra (EADS) of a solution of **1** in 1,2-difluorobenzene containing an excess of complexing dipyriddy fullerene compound **3** ($\lambda_{\text{ex}} = 480$ nm). Global analysis gives lifetimes of 2.3 ps (solid line), 13.6 ps (dashed line), and 230 ps (hollow circles). The inset shows the transient absorption spectrum in the long wavelength region taken 230 ps after excitation. The band is characteristic of the fullerene radical anion.

Spectroscopic Properties of Heptad 1 in 1,2-Difluorobenzene. Having obtained information about the various energy transfer pathways from the study of the model compounds, we now turn our attention to heptad **1**. A solution of **1** was prepared by dissolving hexad **2** in 1,2-difluorobenzene ($\sim 4 \times 10^{-5}$ M) and adding sufficient fullerene ligand **3** to complex essentially all **2**, based on the binding constant of 7.3×10^4 measured for the 1:1 complex in a closely related molecule, which is a complex between dyad **18** (Figure 5) and fullerene **3**.²⁷ This solution, containing **1** and excess **3**, was excited at 480 nm, and the EADS spectra in Figure 11 were obtained. Global analysis of the data gave lifetimes of 2.3, 13.6, and 230 ps. The system involves a variety of excited chromophores, especially at early times, and the EADS do not always represent single chemical species, which complicates the interpretation. However, if these spectra are compared with those obtained for the various simpler model systems, their interpretation becomes clear. The 2.3 ps EADS has features characteristic of BPEA induced absorption at >600 nm and is associated with singlet–singlet energy transfer from BPEA to the porphyrin and to BDPY with some contribution from energy transfer from the most efficient conformations of BDPY to the porphyrin. The 13.6 ps spectrum has broad stimulated emission around 560 nm and ground-state bleaching at 515 nm, both of which are characteristic of BDPY and is thus associated with singlet–singlet energy transfer from less efficient conformations of BDPY to the porphyrin.

Both of these spectra also contain features consistent with the zinc porphyrin radical cation, including induced absorption around 660 nm. Little or no spectral signature of the porphyrin first excited singlet state is observed. This behavior suggests that photoinduced electron transfer from the porphyrin excited singlet state to the fullerene to generate $\text{P}^{+\bullet}\text{-C}_{60}^{\bullet-}$ occurs at a rate faster than or comparable to energy transfer from the antenna system to the porphyrin. Indeed, studies of **18** complexed with **3**²⁷ yield a time constant for photoinduced electron transfer of 3 ps. The presence of the $\text{P}^{+\bullet}\text{-C}_{60}^{\bullet-}$ charge-separated state in **1** is confirmed by the inset in Figure 11, which shows the transient absorption spectrum in the long-wavelength region taken 230 ps after excitation. The maximum in the 1000 nm region is characteristic of the fullerene radical anion. The 230 ps spectrum in the EADS represents the decay of $\text{P}^{+\bullet}\text{-C}_{60}^{\bullet-}$.

The time constants for the various energy and electron transfer processes in heptad **1**, gleaned from the transient experiments on the heptad and model compounds, are given in Table 1.

Discussion

Energetics of the Heptad. In order to interpret the various electron transfer rate constants presented above, the energetics of the excited and charge-separated states must be estimated. The energy of the zinc porphyrin first excited singlet state in **1** is estimated as 2.03 eV from the wavenumber average of the longest-wavelength porphyrin absorption band and the shortest-wavelength emission band in the complex of **2** and ligand **17**. Cyclic voltammetric studies of **3** have given a potential for the first reduction of the fullerene of -0.62 V versus the saturated calomel electrode (SCE). The first oxidation potential of a zinc porphyrin very closely related to that in **1** is 0.75 V versus SCE in benzonitrile.³³ The oxidation potential of the coordinated zinc porphyrins in **1** could be slightly different from this due to ligation of pyridine, which is known to reduce the oxidation potential relative to “uncoordinated” porphyrin,³² and to the distortion of the porphyrin rings and coordination geometry inherent the structure of **1**. Flat porphyrin rings and a 90° angle between the Zn–N bond to pyridyl and the mean porphyrin plane are precluded by strain. The first reduction potential of a model for BDPY is reported as -0.87 V versus SCE.³⁴ From these data, the energy of the $\text{P}^{+\bullet}\text{-C}_{60}^{\bullet-}$ charge-separated state of **1** is estimated as 1.37 eV and that of $\text{BDPY}^{\bullet-}\text{-P}^{+\bullet}$ as 1.62 eV above the ground state. The thermodynamic driving force for formation of $\text{P}^{+\bullet}\text{-C}_{60}^{\bullet-}$ from ^1P is 0.66 eV and that for formation of $\text{BDPY}^{\bullet-}\text{-P}^{+\bullet}$ is 0.41 eV.

Energy Transfer. It is clear from Table 1 that both BPEA and BDPY function as excellent antennas for the porphyrins of **2**, **7**, and **1**. The BPEA moieties absorb in ca. 430–475 nm region between the porphyrin Soret and Q-bands where porphyrin absorption is weak (Figure 2). The BDPY chromophore absorbs in the 475–530 nm region, where BPEA does not absorb, and is well set up energetically to accept singlet excitation energy from BPEA and transfer it to porphyrins. Together, BPEA and BDPY antennas add absorbance in the normally weakly absorbing region between the porphyrin Soret and Q-bands that is larger than the absorbance of the Q-bands themselves at longer wavelengths. In **1**, the combination of the porphyrins and the two types of antenna molecules features absorbance throughout most of the visible spectral region.

Energy transfer from BPEA to BDPY and directly to the porphyrins is very fast relative to decay of $^1\text{BPEA}$ by unichromophoric photophysical processes, and so the quantum yield of energy transfer is essentially unity. In **1** and the hexads, the energy transfer pathways from BPEA to the porphyrins and to the most efficient set of BDPY conformations each occur on the ca. 5 ps time scale, whereas transfer to a slightly less efficient set of conformations of BDPY is slower (14 ps). Energy transfer from $^1\text{BDPY}$ to the porphyrins is also multiexponential, and the fastest process (4–5 ps) is essentially quantitative ($\Phi \geq 0.98$). Transfer by the slower process is slightly less effective, but the quantum yield is still ~ 0.96 . Calculations based on molecular models and using the Förster treatment for singlet–singlet energy transfer yield rate constants consistent with those observed. Thus, overall, the two kinds of chromophores are highly effective antennas for the zinc porphyrins in **1**, transferring energy both directly and by a stepwise mechanism whereby excitation migrates around the hexaphenylbenzene “wheel” from BPEA to BDPY and on to the porphyrin.

There are a few other reports in the literature of singlet–singlet energy transfer from BDPY derivatives to porphyrins. In one of these,³⁴ the rate constant for singlet–singlet energy transfer from a BDPY derivative similar to that in **2** to a covalently linked zinc tetraarylporphyrin was 7–50 times smaller than

those observed for **2**. In that case, only 5 covalent bonds separated the phenyl ring attached to BDPY from that at the meso position on the zinc porphyrin, whereas in **2** there are 9 such bonds. However, the linkage consisted of single bonds, which allow a variety of conformations of the BDPY relative to the porphyrin, many of which would not be favorable for singlet–singlet energy transfer by the Förster mechanism. In **2**, the hexaphenylbenzene core and rigid linkage bonds constrain the BDPY to a region near the porphyrin macrocycle where transfer is favorable. In a second study,³⁰ singlet–singlet energy transfer from a BDPY similar to that in **2** to an attached porphyrin was observed. As with hexad **2**, multiple time constants for energy transfer (ascribed to multiple excited-state conformations) were observed with values of 2.4 and 23 ps for the free base porphyrin and 1.8 and 16 ps for the zinc analog. These molecules featured only an alkynyl group (3 bonds) separating the phenyl ring attached to the BDPY from the meso phenyl ring of the porphyrin, as opposed to the 9 bonds in **2**, yet the energy transfer rates are comparable. This similarity is ascribed to more favorable parameters (interchromophore distances and angles) for Förster singlet–singlet energy transfer in **2** and the other molecules examined in this study. The earlier study invoked a strong contribution from through-bond energy transfer, requiring orbital overlap mediated by the bonds in the interchromophore linkage. The fact that the number of bonds in the linkage is substantially larger for **2** than for the earlier molecules, whereas the singlet–singlet energy transfer rates are comparable, suggests that through-bond contributions are much less important for **2** and its relatives. A small contribution should not be ruled out however as it has been found in related systems that the hexaphenylbenzene core can mediate through-bond energy transfer.²⁵

Electron Transfer. In zinc hexad **2** with no fullerene present, photoinduced electron transfer from the porphyrin first excited singlet states to the BDPY is efficient. Transfer is about twice as fast in 1,2-difluorobenzene containing excess ligand **17** as it is in 2-methyltetrahydrofuran. Two effects may contribute to this difference. The 1,2-difluorobenzene ($\epsilon = 13.8^{35}$) is more polar than 2-methyltetrahydrofuran ($\epsilon = 7.6^{36}$). This should stabilize the charge-separated state in 1,2-difluorobenzene, relative to 2-methyltetrahydrofuran, and in turn increase the driving force for photoinduced electron transfer. This transfer doubtless occurs in the normal region of the Marcus rate constant versus free energy relationship.^{37,38} If the effect of the increase in driving force is larger than any solvent effect on the reorganization energy λ , it will lead to an increase in rate constant. In addition, the pyridine ligand to the zinc decreases the oxidation potential of the porphyrin, and therefore also increases the driving force for electron transfer. We have found that in the noncoordinating solvent dichloromethane, ligation of pyridine to a zinc porphyrin reduces the oxidation potential by 0.11 V.³² Much slower photoinduced electron transfer from a zinc porphyrin to a BDPY has been reported in a system where the electronic coupling between the moieties is much less.³⁴

Charge recombination for **2** in 1,2-difluorobenzene is also more rapid. Charge recombination, with a driving force of ~ 1.6 eV, likely occurs in the “inverted” region of the Marcus relationship. The 1,2-difluorobenzene decreases this driving force by stabilization of the charge-separated state, and increases λ . Additional stabilization of the porphyrin radical cation by pyridine would also occur. These effects would be expected to increase the rate of electron transfer, as is observed.

In heptad **1**, photoinduced electron transfer to the fullerene is extremely rapid, and occurs with a quantum yield of

essentially unity. The yield of photoinduced electron transfer to the BDPY is insignificant. Transfer is substantially faster than has been observed for some other donor–acceptor systems formed by association of a fullerene-bearing nitrogenous group with zinc porphyrins.^{34,39–42} This can be ascribed to good electronic coupling between the porphyrin and fullerene due to the short covalent linkage and the close spatial approach of the moieties. Of course, this same electronic coupling leads to a charge recombination time constant, 230 ps, that, although 70 times larger than the time constant for charge separation, is still smaller than those observed for many porphyrin–fullerene systems with weaker coupling.

Conclusions

Heptad **1** is an artificial photosynthetic antenna–reaction center complex that combines excellent spectral coverage of the visible, highly efficient energy migration from antenna chromophores to the porphyrin by both direct and stepwise pathways, and highly efficient photoinduced electron transfer to yield a charge-separated state with a quantum yield close to unity. The use of self-assembly to couple the electron acceptor to the antenna–donor unit saves a significant amount of synthetic effort but at the expense of having unbound fullerene in the solution that absorbs some of the incident light and converts it to heat. Higher overall efficiencies in an artificial self-assembled system would require very strong, specific binding of the various self-assembling units, as occurs in natural photosynthetic constructs.

Experimental Section

Synthesis and Spectroscopic Studies. The syntheses of **3**,^{43,44} **4**,²⁶ **12**–**16**,²⁶ **17**,^{43,44} and **18**²⁷ have been previously reported. The preparation and characterization of the other molecules used in this study are described in detail in the Supporting Information, as are the various experimental setups for the spectroscopic measurements.

Acknowledgment. This work was supported by a grant from the U.S. Department of Energy (DE-FG02-03ER15393).

Supporting Information Available: Experimental details of the synthesis and spectroscopic investigations. This material is available free of charge via the Internet at <http://pubs.acs.org>.

References and Notes

- (1) Kodis, G.; Liddell, P. A.; de la Garza, L.; Clausen, P. C.; Lindsey, J. S.; Moore, A. L.; Moore, T. A.; Gust, D. *J. Phys. Chem. A* **2002**, *106*, 2036–2048.
- (2) Kuciauskas, D.; Liddell, P. A.; Lin, S.; Johnson, T. E.; Weghorn, S. J.; Lindsey, J. S.; Moore, A. L.; Moore, T. A.; Gust, D. *J. Am. Chem. Soc.* **1999**, *121*, 8604–8614.
- (3) Aratani, N.; Osuka, A.; Kim, Y. H.; Jeong, D. H.; Kim, D. *Angew. Chem., Int. Ed.* **2000**, *39*, 1458–1462.
- (4) Bothner-By, A. A.; Dadok, J.; Johnson, T. E.; Lindsey, J. S. *J. Phys. Chem.* **1996**, *100*, 17551–17557.
- (5) Burrell, A. K.; Officer, D. L.; Plieger, P. G.; Reid, D. C. W. *Chem. Rev.* **2001**, *101*, 2751–2796.
- (6) Guldi, D. M. *Chem. Soc. Rev.* **2002**, *31*, 22–36.
- (7) Harriman, A. Energy transfer in synthetic porphyrin arrays. In *Supramolecular Photochemistry*; Balzani, V., Ed.; D. Reidel Publishing Company: Dordrecht, Holland, 1987; pp 207–223.
- (8) Li, J.; Ambrose, A.; Yang, S. I.; Diers, J. R.; Seth, J.; Wack, C. R.; Bocian, D. F.; Holten, D.; Lindsey, J. S. *J. Am. Chem. Soc.* **1999**, *121*, 8927–8940.
- (9) Li, J.; Diers, J. R.; Seth, J.; Yang, S. I.; Bocian, D. F.; Holten, D.; Lindsey, J. S. *J. Org. Chem.* **1999**, *64*, 9090–9100.
- (10) Lin, V. S. Y.; Dimagno, S. G.; Therien, M. J. *Science* **1994**, *264*, 1105–1111.
- (11) Nakano, A.; Osuka, A.; Yamazaki, I.; Yamazaki, T.; Nishimura, Y. *Angew. Chem., Int. Ed.* **1998**, *37*, 3023–3027.

- (12) Paolesse, R.; Jaquinod, L.; Della Sala, F.; Nurco, D. J.; Prodi, L.; Montalti, M.; Di Natale, C.; D'Amico, A.; Di Carlo, A.; Lugli, P.; Smith, K. M. *J. Am. Chem. Soc.* **2000**, *122*, 11295–11302.
- (13) Rucareanu, S.; Mongin, O.; Schuwey, A.; Hoyler, N.; Gossauer, A.; Amrein, W.; Hediger, H.-U. *J. Org. Chem.* **2001**, *66*, 4973–4988.
- (14) Cho, H. S.; Rhee, H.; Song, J. K.; Min, C.-K.; Takase, M.; Aratani, N.; Cho, S.; Osuka, A.; Joo, T.; Kim, D. *J. Am. Chem. Soc.* **2003**, *125*, 5849–5860.
- (15) Brodard, P.; Matzinger, S.; Vauthey, E.; Mongin, O.; Papamicaël, C.; Gossauer, A. *J. Phys. Chem. A* **1999**, *103*, 5858–5870.
- (16) Hwang, I.-W.; Kamada, T.; Ahn, T. K.; Ko, D. M.; Nakamura, T.; Tsuda, A.; Osuka, A.; Kim, D. *J. Am. Chem. Soc.* **2004**, *126*, 16187–16198.
- (17) Morandeira, A.; Vauthey, E.; Schuwey, A.; Gossauer, A. *J. Phys. Chem. A* **2004**, *108*, 5741–5751.
- (18) Nakamura, Y.; Hwang, I.-W.; Aratani, N.; Ahn, T. K.; Ko, D. M.; Takagi, A.; Kawai, T.; Matsumoto, T.; Kim, D.; Osuka, A. *J. Am. Chem. Soc.* **2005**, *127*, 236–246.
- (19) Aratani, N.; Osuka, A.; Cho, H. S.; Kim, D. *J. Photochem. Photobiol., C* **2002**, *3*, 25–52.
- (20) Bensasson, R. V.; Land, E. J.; Moore, A. L.; Crouch, R. L.; Dirks, G.; Moore, T. A.; Gust, D. *Nature (London)* **1981**, *290*, 329–332.
- (21) Gould, S. L.; Kodis, G.; Liddell, P. A.; Palacios, R. E.; Brune, A.; Gust, D.; Moore, T. A.; Moore, A. L. *Tetrahedron* **2006**, *62*, 2074–2096.
- (22) Kodis, G.; Herrero, C.; Palacios, R.; Mariño-Ochoa, E.; Gould, S. L.; de la Garza, L.; van Grondelle, R.; Gust, D.; Moore, T. A.; Moore, A. L.; Kennis, J. T. M. *J. Phys. Chem. B* **2004**, *108*, 414–425.
- (23) Macpherson, A. N.; Liddell, P. A.; Kuciauskas, D.; Tatman, D.; Gillbro, T.; Gust, D.; Moore, T. A.; Moore, A. L. *J. Phys. Chem. B* **2002**, *106*, 9424–9433.
- (24) Berera, R.; van Stokkum, I. H. M.; Kodis, G.; Keirstead, A. E.; Pillai, S.; Herrero, C.; Palacios, R. E.; Vengris, M.; van Grondelle, R.; Gust, D.; Moore, T. A.; Moore, A. L.; Kennis, J. T. M. *J. Phys. Chem. B* **2007**, *111*, 6868–6877.
- (25) Kodis, G.; Terazono, Y.; Liddell, P. A.; Andréasson, J.; Garg, V.; Hambourger, M.; Moore, T. A.; Moore, A. L.; Gust, D. *J. Am. Chem. Soc.* **2006**, *128*, 1818–1827.
- (26) Terazono, Y.; Liddell, P. A.; Garg, V.; Kodis, G.; Brune, A.; Hambourger, M.; Moore, T. A.; Moore, A. L.; Gust, D. *J. Porphyrins Phthalocyanines* **2005**, *9*, 706–723.
- (27) Terazono, Y.; Kodis, G.; Liddell, P. A.; Garg, V.; Gervald, M.; Moore, T. A.; Moore, A. L.; Gust, D. *Photochem. Photobiol.* **2007**, *83*, 464–469.
- (28) Magde, D.; Wong, R.; Seybold, P. G. *Photochem. Photobiol.* **2002**, *75*, 327–334.
- (29) Kee, H. L.; Kirmaier, C.; Yu, L. H.; Thamvongkit, P.; Youngblood, W. J.; Calder, M. E.; Ramos, L.; Noll, B. C.; Bocian, D. F.; Scheidt, W. R.; Birge, R. R.; Lindsey, J. S.; Holten, D. *J. Phys. Chem. B* **2005**, *109*, 20433–20443.
- (30) Li, F.; Yang, S. I.; Ciringh, Y.; Seth, J.; Martin, C. H.; Singh, D.; Kim, D.; Birge, R. R.; Bocian, D. F.; Holten, D.; Lindsey, J. S. *J. Am. Chem. Soc.* **1998**, *120*, 10001–10017.
- (31) Förster, T. *Disc. Faraday Soc.* **1959**, *27*, 7–17.
- (32) Gust, D.; Moore, T. A.; Moore, A. L.; Kang, H.-K.; DeGraziano, J. M.; Liddell, P. A.; Seely, G. R. *J. Phys. Chem.* **1993**, *97*, 13637–13642.
- (33) Liddell, P. A.; Kodis, G.; de la Garza, L.; Moore, A. L.; Moore, T. A.; Gust, D. *J. Phys. Chem. B* **2004**, *108*, 10256–10265.
- (34) D'Souza, F.; Smith, P. M.; Zandler, M. E.; McCarty, A. L.; Itou, M.; Araki, Y.; Ito, O. *J. Am. Chem. Soc.* **2004**, *126*, 7898–7907.
- (35) Mansingh, A.; Mclay, D. B. *J. Chem. Phys.* **1971**, *54*, 3322.
- (36) Reichardt, C. *Solvent Effects in Organic Chemistry*; Verlag Chemie: New York, 1979.
- (37) Marcus, R. A. *J. Chem. Phys.* **1956**, *24*, 966–978.
- (38) Marcus, R. A.; Sutin, N. *Biochim. Biophys. Acta* **1985**, *811*, 265–322.
- (39) D'Souza, F.; Deviprasad, G. R.; Zandler, M. E.; Hoang, V. T.; Klykov, A.; VanStipdonk, M.; Perera, A.; El Khouly, M. E.; Fujitsuka, M.; Ito, O. *J. Phys. Chem. A* **2002**, *106*, 3243–3252.
- (40) D'Souza, F.; Deviprasad, G. R.; Zandler, M. E.; El Khouly, M. E.; Fujitsuka, M.; Ito, O. *J. Phys. Chem. A* **2003**, *107*, 4801–4807.
- (41) D'Souza, F.; Ito, O. *Coord. Chem. Rev.* **2005**, *249*, 1410–1422.
- (42) D'Souza, F.; Chitta, R.; Gadde, S.; Islam, D.-M. S.; Schumacher, A. L.; Zandler, M. E.; Araki, Y.; Ito, O. *J. Phys. Chem. B* **2006**, *110*, 25240–25250.
- (43) Habicher, T.; Nierengarten, J. F.; Gramlich, V.; Diederich, F. *Angew. Chem., Int. Ed.* **1998**, *37*, 1916–1919.
- (44) Bourgeois, J. P.; Woods, C. R.; Cardullo, F.; Habicher, T.; Nierengarten, J. F.; Gehrig, R.; Diederich, F. *Helv. Chim. Acta* **2001**, *84*, 1207–1226.

JP900835S